Comparison of the self-healing behaviour of 60Sn40Pb and 99.3Sn0.7Cu solder alloy reinforced Al6061 MMCs'.

MANTHA, S.R.V., KUMAR, G.B.V., PRAMOD, R., RAO, C.S.P., SAHARUDIN, M.S. and SAHU, S.K.

2025

Journal of
Manufacturing and Materials Processing

Article

Comparison of the Self-Healing Behaviour of 60Sn40Pb and 99.3Sn0.7Cu Solder Alloy Reinforced Al6061 MMCs'

Subrahmanya Ranga Viswanath Mantha [1,2], Gonal Basavaraja Veeresh Kumar [1,*], Ramakrishna Pramod [3], Chilakalapalli Surya Prakasha Rao [4], Mohd Shahneel Saharudin [5,*] and Santosh Kumar Sahu [6,*]

[1] Department of Mechanical Engineering, National Institute of Technology-Andhra Pradesh, Tadepalligudem 534101, India
[2] Department of Mechanical Engineering, Vignan's Institute of Information Technology, Visakhapatnam 530049, India
[3] Department of Mechanical Engineering, Amrita Vishwa Vidyapeetham, Bengaluru 560035, India
[4] Department of Mechanical Engineering, National Institute of Technology-Warangal, Warangal 506004, India
[5] School of Computing & Engineering Technology, Robert Gordon University, Garthdee Road, Aberdeen AB10 7QB, UK
[6] School of Mechanical Engineering, VIT-AP University, Besides A.P. Secretariat, Amaravati 522237, India
* Correspondence: veereshkumargb@nitandhra.ac.in (G.B.V.K.); s.saharudin@rgu.ac.uk (M.S.S.); sksahumech@gmail.com (S.K.S.)

Abstract: The self-healing characteristics of Al6061 reinforced with CuO have been examined experimentally. The solder alloys 60Pb40Sn and 99.3Sn0.7Cu with low melting points are incorporated to strengthen the Al6061 MMCs'; the self-healing properties have been investigated. Developed self-healing samples have undergone testing for hardness, tensile, and impact characteristics in accordance with ASTM standard test protocols. The findings demonstrate how the solder filling affects the mechanical characteristics of self-healed Al6061 alloy and its MMCs'. The results showed that the composites formed a decent bond between the solder and matrix, confirming successful fabrication. Pb-Sn filled samples demonstrated higher self-healing efficiency for tensile and impact of 90.02% and 90.30% with 6 wt.% of CuO, respectively, and Sn-Cu filled samples witnessed higher self-healing efficiency for tensile and impact of 91.81% and 91.09% with 6 wt.% of CuO respectively. However, the self-healed composite did not split in two when subjected to Charpy impact and tensile strength tests, and the healing efficiency of Sn-Cu-filled composites is higher than that of the Pb-Sn-filled composites.

Keywords: Al6061-CuO MMCs'; Self-healing; 60Sn40Pb; 99.3Sn0.7Cu; solder; low melting point alloy

check for updates

Academic Editors: Daniel F.O. Braga and Sérgio Tavares

Received: 16 March 2025
Revised: 17 April 2025
Accepted: 22 April 2025
Published: 24 April 2025

Citation: Mantha, S.R.V.; Kumar, G.B.V.; Pramod, R.; Rao, C.S.P.; Saharudin, M.S.; Sahu, S.K. Comparison of the Self-Healing Behaviour of 60Sn40Pb and 99.3Sn0.7Cu Solder Alloy Reinforced Al6061 MMCs'. *J. Manuf. Mater. Process.* **2025**, *9*, 141. https://doi.org/10.3390/jmmp9050141

1. Introduction

The ability to attain a range of property combinations not offered by conventional monolithic materials has sparked an increase in interest in the design and development of composite materials [1]. Aluminium Metal Matrix Composites (Al-MMCs) remain the most studied and widely used Metal Matrix Composites (MMCs) because of their easy manufacturing, attractive properties, and ease of post-fabrication heat treatment [1,2].

Al-MMCs produced encouraging outcomes in improving physical, mechanical, and tribological properties [3–5] and thoroughly examining processing factors, including reinforcement size and shape, processing methodology, and control variables [6]. MMCs are often produced by squeeze casting [7], powder metallurgy [8], and liquid state casting [9] for a variety of uses in the recreation, automobile, aerospace, military, and marine sectors [10,11]. The most widely used technique for economically generating Al-MMCs persists in stir casting [10]. This method uses continuous ceramic fibres or discontinuous particles to reinforce the matrix material in a liquid state [12]. Although the method is widely known, the porosity found in these materials raises severe concerns [13,14]. Poor interfacial bonding among the alloy matrix and particulate reinforcing material causes porosity in Al-MMCs, which might be the starting point for corrosion and mechanical problems.

According to earlier research, the interfacial bonding among the particulate ceramic reinforcements and the alloy matrix may be enhanced in stir-cast composites by adjusting the stirring duration and speed and employing Magnesium (Mg) as a wetting agent [14]. Porosity reduction in composites has also been reported to be achieved by post-fabrication deformation, careful reinforcing material selection, and combinations of two or more reinforcing materials. Nonetheless, the conventional preventative management model still encompasses these initiatives. The materials finally fail due to damage development [15], a disadvantage of the old preventative management philosophy in material processing. A novel self-healing strategy is designed to address material damage from defects such as porosity, microcracks, or flaws during operational use, mirroring the natural wound-sealing process of blood clotting in biological systems.

Self-healing material development is a challenging and crucial process. However, one of the most innovative materials is being considered due to recent advancements in materials technology and is based on biological ideas in living things, i.e., self-healing [16–20]. The ability of living organisms to self-heal is to fix or restore damage on their own. Incorporating self-healing principles into commercial material processing has several benefits, including increased material service life, reduced downtime in industrial processes, and cheaply producing self-healing materials [21–23]. By using this bio-mimics method, researchers worldwide are developing innovative materials with self-healing features to improve the materials' use, longevity and performance.

These advantages have made significant advancements in manufacturing polymers and polymer-based composites with self-healing capabilities possible [24]. Similarly, several publications have documented ceramics and ceramic-based composites' capacity for self-healing [25]. Nonetheless, the field of self-healing is still little understood, and as a result, its economic use is still somewhat restricted. Strong bonding and slower diffusion rates are why self-healing properties in metallic systems and MMCs have not been widely documented. These self-healing methods have a high enough diffusion rate compared to polymers to fill damaged nucleation sites, including micro gaps and fractures, by healing agents [15]. Composites are composed of ceramic components reinforced with metallic alloys, increasing the porosity of the materials. Since porosity acts as a nucleation site for failures in material systems used for structural applications, using self-healing design principles as a damage control strategy becomes interesting if catastrophic failures are to be avoided.

Developing the ability of metals to heal themselves is being accomplished in three very different ways: (i) filling cracks with supersaturated solid solution precipitates, (ii) adding shape memory alloy (SMA) in the form of wires to metallic matrices, and (iii) reinforcing metallic matrices with low-melting-point alloys [26,27]. In previous attempts, a compositional matrix of Sn-13% Bismuth (Bi) self-healing is attained by incorporating Nitinol wires of 1 volume fraction [28]. Another study used solution hardening and age hardening as a strength model and found that the strength increased for magnesium (5.7 weight per cent), zinc (Zn) (2.7 weight per cent), and aluminium (Al) reinforced with nitinol wire [29]. An additional study on the A380 matrix's self-healing capabilities was conducted using nitinol wire [30]. Zinc alloy ZA-8 matrix reinforced with nitinol wire cast by various loading techniques (direct and indirect). Indirect load transfer was significantly more effective in achieving complete fracture closure and recovering Ultimate Tensile Strength (UTS) by up to 30% [31].

Al6061 is widely used in engineering applications due to its fluidity, castability, corrosion resistance, and adequate strength-to-weight ratio. This is especially true in the transportation and construction industries, where reinforced Al-MMCs are primarily sought for superior mechanical qualities like tensile strength and hardness [32]. When CuO was added to the Al6061 matrix, density, hardness, and tensile yield strength increased noticeably. The cumulative impact of many strengthening mechanisms offered by the CuO reinforcements is responsible for these improvements [33].

Material scientists have recently shown great interest in using alloys with lower melting points (solders) to create self-healing. Alloys with a lower melting point melt and flow to fill the crack site when heated to healing temperatures. After that, they harden and mend the fissures, giving intrinsic self-healing properties to the substance [34,35]. The healing effectiveness of this approach is encouraging, and a strength regain of around 60% of the initial damage strength is attainable. Using the Charpy impact test, Oladijio et al. [36] examined self-healed Al-hybrid MMCs' impact properties. The Al-hybrid MMC with self-healing was created using a reinforced alloy with a lower melting point. Scientists noted that because of the self-healing procedure, the energy absorbed by the repaired samples displayed enhancement over the damaged ones. The maximum healing efficiency achieved is 61%. This self-healing technique has been investigated in a few metallic systems, including Al alloy with Sn60Pb40 solder. Using Sn60Pb40 as a solder resulted in a 91% self-healing efficiency in the Alaneme and Omosule work [15]. Due to the high expense of using SMA as metal reinforcing elements, this investigation concentrates on low melting point alloys as an inexpensive method of producing self-healing in Al-based composites.

This study chose Al alloy 6061 (Al6061) as the base alloy material due to its outstanding mechanical properties, corrosion resistance, widespread use in structural and electronic applications, and CuO as the primary reinforcing material. To evaluate the impact of different soldering materials on Al6061-CuO, two distinct solder alloys, 60Pb40Sn and 99.3Sn0.7Cu, were utilized. These solders were chosen based on their compatibility with Al, mechanical strength, and thermal performance. The comparative analysis of Al6061-CuO + Pb-Sn and Al6061-CuO + Sn-Cu aims to determine the most suitable solder for optimizing joint reliability, mechanical integrity, and microstructural stability in Al-MMCs' applications.

2. Materials and Methodology

2.1. Matrix and Reinforcement

CuO is the primary reinforcing element in this study, while Al-Mg-Si alloy is the matrix. Low melting point solders were used as secondary reinforcing material (self-healing agent) to test two distinct solders, 60Sn-40Pb (Pb-Sn) and 99.3Sn-0.7Cu (Sn-Cu). Table 1 lists the chemical composition of the Al-Mg-Si (Al6061) alloy, which was purchased from Bharat Aerospace Metals Ltd. in Mumbai. Sigma Aldrich provided the CuO particles, which had an average size of 50 µm. Table 2 lists the alloy and CuO characteristics.

Table 1. Chemical composition of Al6061 alloy.

Chemical Composition (wt.%)	Ti	Mn	Cr	Fe	Si	Zn	Cu	Mg	Al
Al6061	0.01	0.03	0.22	0.23	0.62	0.10	0.22	0.84	Bal

Table 2. Characteristics of Al6061 and reinforcement CuO particulates.

Property	Thermal Conductivity (W/mk)	Coefficient Thermal Expansion (/K)	Melting Point (°C)	Density (g/cc)	Modulus of Elasticity (Gpa)
Al6061	200	23.6×10^{-6}	600	2.7	69.5
CuO	69–75	5.5×10^{-6}	1326	6.31	81.6

2.2. Production of Composites

The CuO-reinforced Al6061 composites are produced via a bottom-poured stir-casting method with ultrasonic assistance, which is made possible by Chennai-based Swam equipment. To prevent oxidation, inert gas shielding is employed, the reinforcement is preheated to 500 °C to reduce the thermal mismatch among the particulate reinforcement and alloy matrix, and superior castings with improved reinforcement distribution are produced using gravity-based casting. CuO reinforcements were added to Al6061 in weight increments of 0 to 6 weight per cent in steps of two in order to create Al-MMCs′. Table 3 provides an overview of the terminology and the elements that comprise the combination. For the Al6061 ingots to fit within the crucible, they were first chopped into smaller sizes. The CuO particulates were heated to 500 °C in the furnace to eliminate moisture and reduce the temperature difference between the molten metal and the reinforcement. The molten matrix is placed in a crucible, maintained at 770 °C, and then correctly agitated for 10 min at 500 rpm using a steel stirrer coated with graphite paste to maintain a constant temperature during the melt process. After five minutes of stirring, a long metal funnel was used to feed the measured, heated CuO powder to the molten matrix at 2–3 g per minute. Ten minutes of swirling the molten metal guarantees that the warmed CuO particles are distributed evenly throughout the fluid, enhancing mixing. CuO reinforcement particles were placed directly in the formed vortex caused by the whirling of the molten metal. In order to achieve homogenous dispersion, the clusters of the CuO reinforcement particles were broken by using an ultrasonic vibrator set to 20 kHz for five minutes.

Table 3. Nomenclature of Al6061-CuO MMCs filled with Pb-Sn/Sn-Cu solder.

	Reinforcement	Nomenclature
Solder	Pb-Sn	6C0Pb-Sn, 6C1Pb-Sn,6C2Pb-Sn, 6C3Pb-Sn
	Sn-Cu	6C0Sn-Cu, 6C1Sn-Cu, 6C2Sn-Cu, 6C3Sn-Cu

The inclusion of Mg chips in the mixture was intended to improve the wettability of the CuO reinforcement particle, release gases that were encapsulated inside the melt, and avoid the cast becoming permeable. Forty grams of hexachloroethane (C_2CL_6) were utilized to remove the gas from the melt. After 10 min, they were stirred up once more. Molten metal enters the mould box's heated, graphite-coated cylinders, which are 120 mm in length and 8 mm in radius, via the bottom of the furnace to cool naturally to room temperature. The entire procedure is carried out in an isolated environment using argon gas to avoid the formation of oxides. Likewise, the ultrasonic-assisted stir-casting technique was used to produce further series composites. The weight percentage of CuO is taken as 0, 2, 4, and 6 for the Al6061, which are designated as 6C0, 6C1, 6C2, and 6C3, respectively.

2.3. Low Melting Point Alloy (Solder)

Two low melting alloys (solders) in wire form, i.e., Pb-Sn and Sn-Cu, were used as secondary reinforcement for self-healing study and procured from Hybrid Metals Pvt

Ltd., Bangalore, India. The melting points of Pb-Sn and Sn-Cu are at 183 °C and 227 °C, respectively. The SEM images of the solders are presented in Figure 1a,b. The solders are filled into the composites by drilling a hole of 3 mm; as presented in Figure 1c,d, the self-healing composites were created [16]. In order to reduce the thermal mismatch, the composite was heated for 10 min at 280 °C, whereas soldiers were poured at 230 °C. Then, a set of test specimens with typical geometric forms and sizes was made to examine the mechanical and physical characteristics. The nomenclature of the solder-filled samples is presented in Table 3.

(**a**)

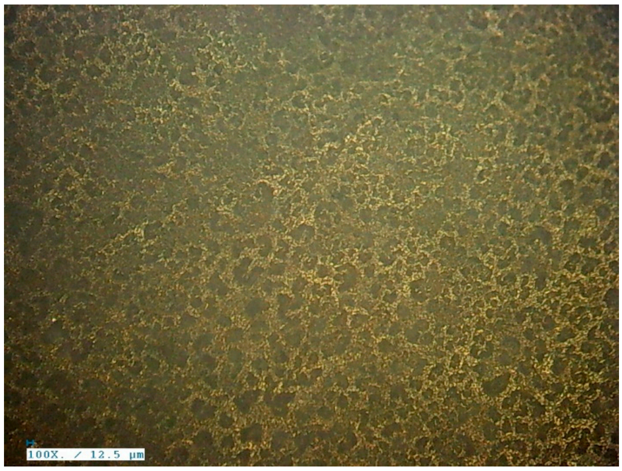

(**b**)

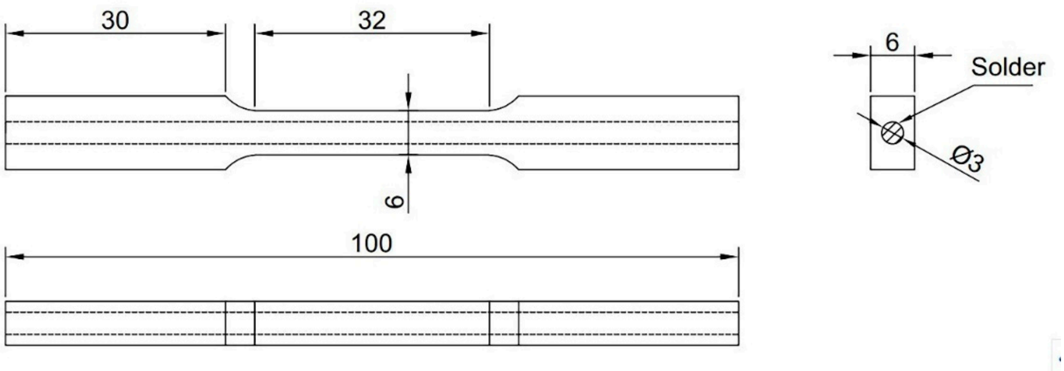

(**c**)

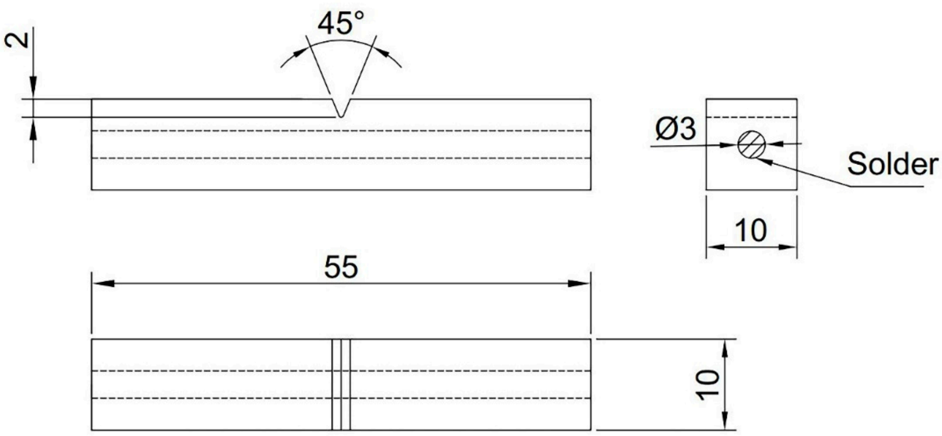

(**d**)

Figure 1. (**a**) 60Pb40Sn solder, (**b**) 99.3Sn0.7Cu solder, (**c**) Tensile specimen drawing filled with solder, (**d**) Impact specimen drawing filled with solder.

2.4. Characterization

The standard ASTM test protocols were used to establish the physical parameters of developed self-healing Al6061 alloy and MMCs. The test samples' hardness, tensile strength, rupture energy, and other characteristics were evaluated using the Hardness, Tensile, and Charpy tests. The Pb-Sn and Sn-Cu solder reinforcements were applied independently to the test specimens. A 3 mm through hole was drilled into them to strengthen the test specimens, and Pb-Sn and Sn-Cu alloy were subsequently poured into them. After that, an Optical Microscope (OM) was used to analyze the manufactured samples and determine whether the cavity was filled correctly. The samples were polished for each test using emery paper with a grain size of up to 1200 and etched using Keller's reagent for matrix and a solution of Nitric Acid diluted in alcohol (typically 10% nitric acid in 90% ethanol) for solder individually. Before and after every test, the specimens were cleaned with acetone. Micrographs were obtained at Virtue Meta Solutions in Hyderabad using an OM. According to ASTM E10-07a, hardness testing uses the Vicker hardness testing equipment. According to the ASTM E-23-07, ASTM E8 M15 was utilized for the Ultimate Tensile Strength (UTS) and elongation% in an Instron machine and Charpy test utilizing Tinius Olsen. Each reading that is presented here is an average of five readings. To ensure the data collected was reliable and repeatable, repeat tests were conducted for every test scenario.

2.5. Self-Healing Experimental Studies

The Pb-Sn and Sn-Cu solders were filled into holes of ϕ3 mm diameter bored longitudinally in the test samples as per the drawing presented in Figure 1c,d to conduct investigations on the healing caused by the insertion of secondary reinforcement (solder).

2.5.1. Self-Healing Test for Tensile Test Species

A ϕ1 mm hole was bored on the surface of three tensile test specimen samples to pass through the solder inserted in the composite. This was done to mimic the creation of mechanical damage-cracks on the MMCs. The test samples' tensile characteristics were then evaluated after exposure to tensile fracture. These pre-cracked samples, also known as damaged samples, were subjected to tensile tests. In order to prevent the solder from draining during heating, another set of cracked solder-reinforced composite samples was constructed. This time, they were wrapped in aluminium foil, heated to 240 °C for 15 min, and cooled naturally in the surrounding air. These samples were called "healed samples" after undergoing tensile testing to check for fractures. Finally, tensile testing is performed on a different set of solder-filled samples called virgin specimens that have never been cracked. The samples' specifics are listed in Figure 2a. Every tensile test was conducted in accordance with ASTM guidelines. Every sample was tested for tensile strength, and the tensile strength was noted and utilized to calculate the healing efficiency. Each composition underwent three repetitions of the test to ensure the reliability and repeatability of the findings.

2.5.2. Self-Healing Test for Charpy Test Specimen

The low melting point solder included in the Al matrix was penetrated by a ϕ1 mm pre-cracked hole bored 0.3 mm from the radius of the 45° notch in one set of samples. This was done to mimic the emergence of cracks on the composites. Impact tests were performed on the test samples. The term "damaged samples" was used to describe this group of previously fractured samples. Healed samples are a different set of pre-cracked composite samples wrapped in Al foil (wrapping in foil is to prevent the solder from draining during heating) on both ends and heated to 240 °C for 15 min before being allowed to cool naturally.

Lastly, virgin samples not previously cracked were also made and tested. The details of the samples are mentioned in Figure 2b. Every impact test was conducted in accordance with ASTM guidelines. Impact testing was performed on each sample, and the energy absorbed was measured and utilized to calculate the healing efficiency. To guarantee the accuracy and consistency of the results, the test was run three times for each mixture.

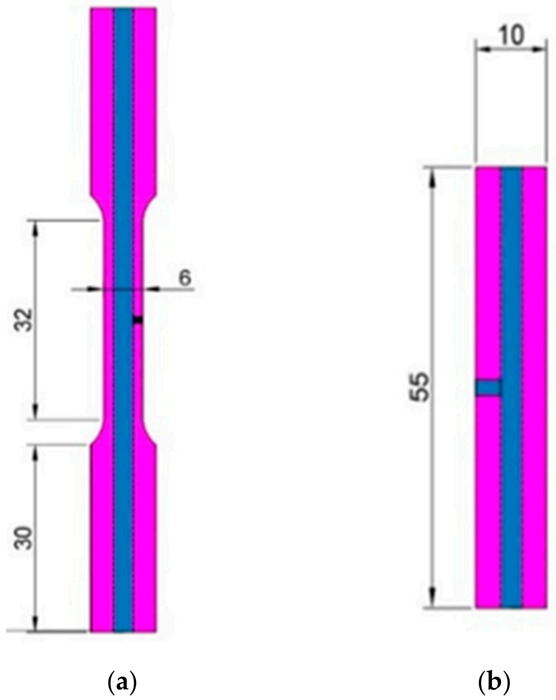

Figure 2. (**a**) Self-healing tensile test samples, (**b**) Self-healing impact test samples.

Using Equation (1), the efficiency attained by self-healing with both treatments was calculated [15,37].

$$\eta_{Self\ Healing} = P_{Healed}/P_{Virgin} * 100 \quad (1)$$

Equation (1) is utilized to compute the efficiency of self-healing ($\eta_{Self\ Healing}$) of the test samples with P denotes the Performance parameter, the Performance parameter for the healed specimen is denoted by P_{Healed}, whereas the P_{Virgin} For virgin specimens. The Performance parameters used for efficiency calculations are UTS and impact energy absorbed. In the current study, the parameters chosen are UTS and impact energy absorbed.

3. Results and Discussions

3.1. Microstructural Studies for Samples Incorporated with Solders

The microstructures of the Pb-Sn and Sn-Cu filled in Al6061-CuO composites were examined, and a satisfactory bond between solder (dark phase) with the matrix (lighter phase) was achieved, as shown in macrograph Figure 3a,b. It is evident from the micrographs that a decent bond is formed between solder and composites, which confirms the successful fabrication of composites. Figure 3c–f presents the micrographs of the matrix-solder interface for Pb-Sn sold-filled composites, and Figure 3g–j presents the micrographs of the matrix-solder interface for Sn-Cu sold-filled composites. Figure 3k,l presents the micrographs of the solder filling cracks.

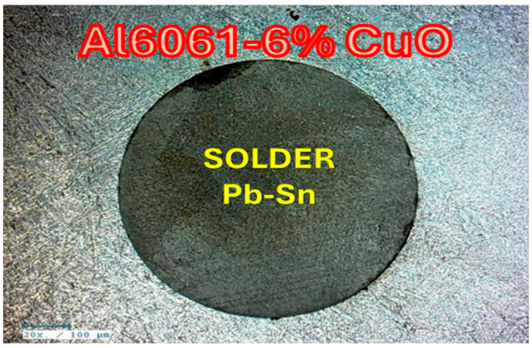

(**a**) 6C3Pb-Sn sample

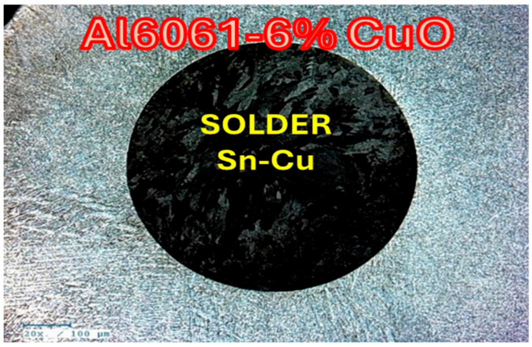

(**b**) 6C3Sn-Cu sample

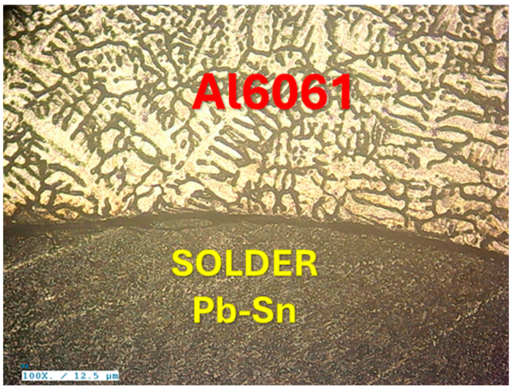

(**c**) 6C0Pb-Sn matrix and solder interface

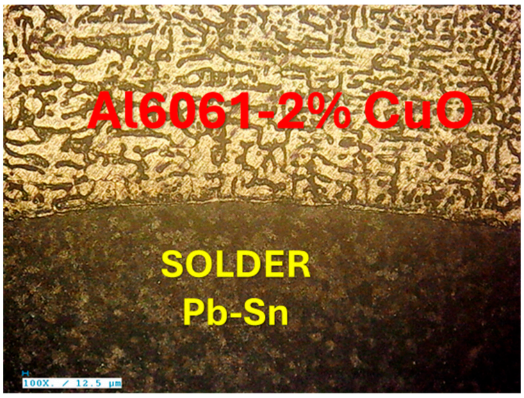

(**d**) 6C1Pb-Sn matrix and solder interface

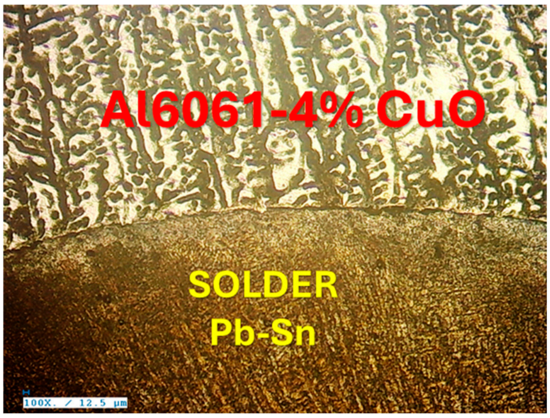

(**e**) 6C2Pb-Sn matrix and solder interface

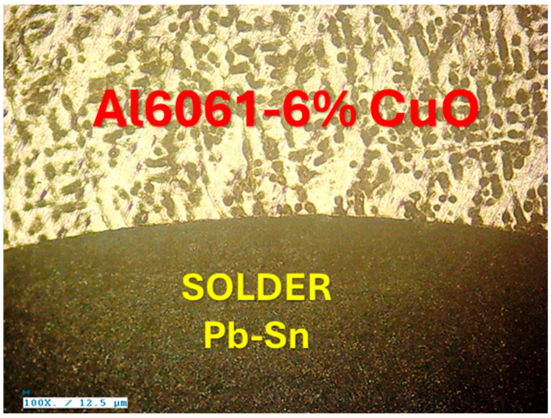

(**f**) 6C3Pb-Sn matrix and solder interface

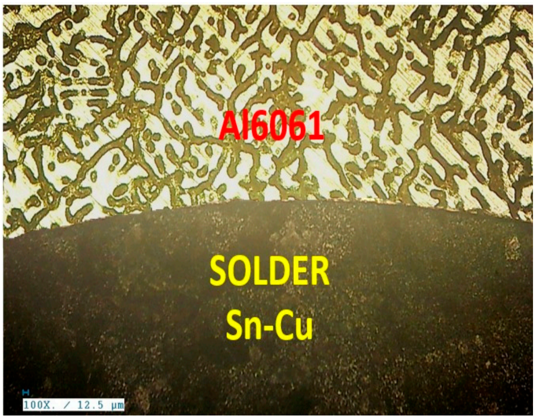

(**g**) 6C0Sn-Cu matrix and solder interface

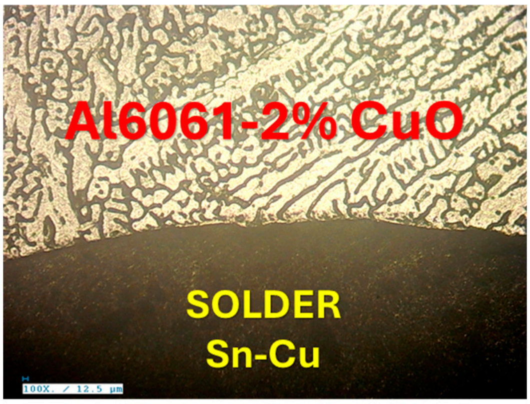

(**h**) 6C1Sn-Cu matrix and solder interface

Figure 3. *Cont.*

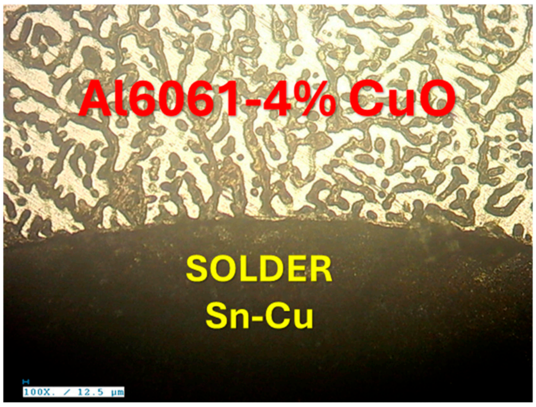

(**i**) 6C2Sn-Cu matrix and solder interface

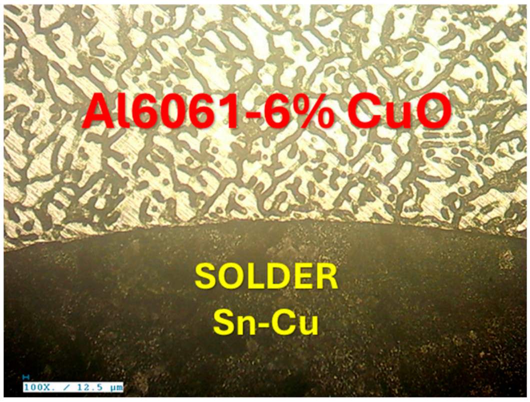

(**j**) 6C3Sn-Cu matrix and solder interface

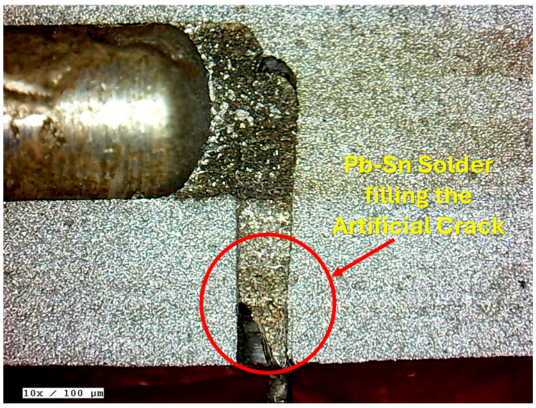

(**k**) Pb-Sn Solder filling the Artificial crack

(**l**) Sn-Cu Solder filling the Artificial crack

Figure 3. (**a**,**b**) Macrograph of the of 6C3Pb-Sn and 6C3Sn-Cu, (**c**–**f**) Micrographs of matrix-solder interface for Pb-Sn sold filled composites, (**g**–**j**). Micrographs of matrix-solder interface for Sn-Cu solder-filled composites (**k**,**l**) Micrographs of the solder filling cracks.

3.2. Hardness for Samples Incorporated with Solders

The hardness is tested on the samples along the diameter of the cross-section to measure hardness on the base material, interface and solder. The hardness of the interface is observed to be greater than that of the solder. Figure 4 represents the hardness of the sample due to the reinforcement. The hardness of the MMCs increased with the increase in CuO filler content, which is the highest at 6 wt.%. It is observed that hardness is higher for composites than interface and lowest for solder. The hardness at the interface of Pb-Sn solder-filled composites is higher than that of Sn-Cu solder-filled composites.

3.3. Al6061-CuO MMCs Filled with Solders Yield Strength, UTS and Elongation

The tensile test samples were prepared and presented in Figure 5a, and the radiography test image (Figure 5b) confirmed the filling of solder in gauge length. Further samples with incomplete filling were again properly filled and tested.

The Yield strength for Pb-Sn reinforced samples for base alloy (6C0Pb-Sn) for the virgin test specimen is 141.73 MPa as compared to that of the self-healed sample is 107.99 MPa respectively, whereas the yield strength for 6 wt.% of CuO (6C3Pb-Sn) reinforced virgin sample is 235.55 MPa. The healed sample is 206.547 MPa. The results are presented in the graph in Figure 6a. In contrast, yield strength for Sn-Cu reinforced samples with base alloy (6C0Sn-Cu) for the virgin test specimen is 145.83 MPa as compared to that of the self-healed sample is 112.64 MPa, the Yield strength for 6 wt.% of CuO (6C3Sn-Cu) reinforced virgin sample is 242.79 MPa and healed samples is 226.56 MPa, Figure 6b is presented with the results. The standard deviation for UTS strength of Pb-Sn and Sn-Cu filled Al6061-CuO MMCs Sn-Cu solder was ±7.12 MPa and ±6.93 MPa.

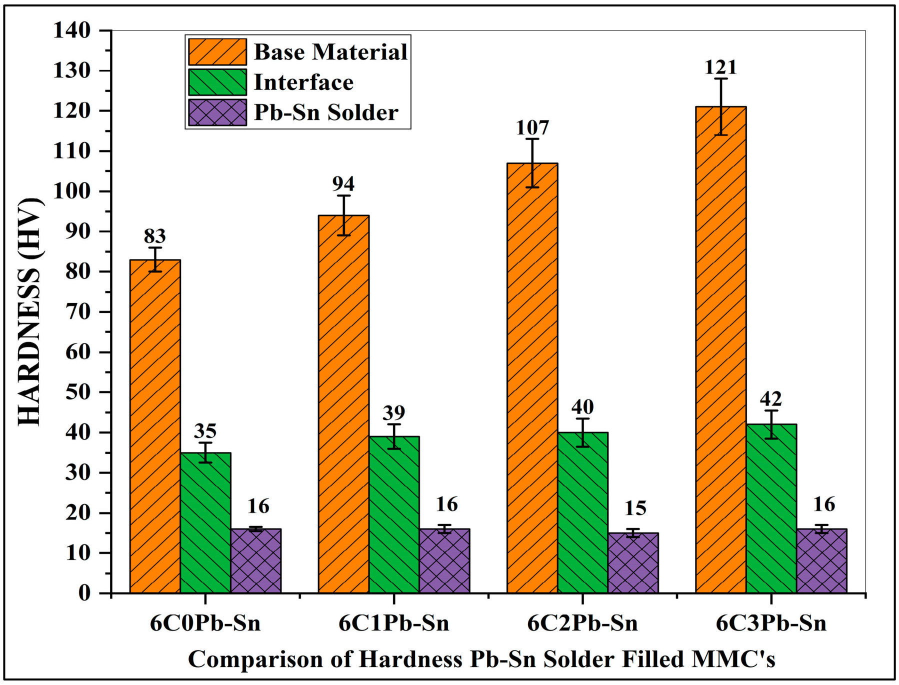

(**a**) Pb-Sn solder filled samples hardness

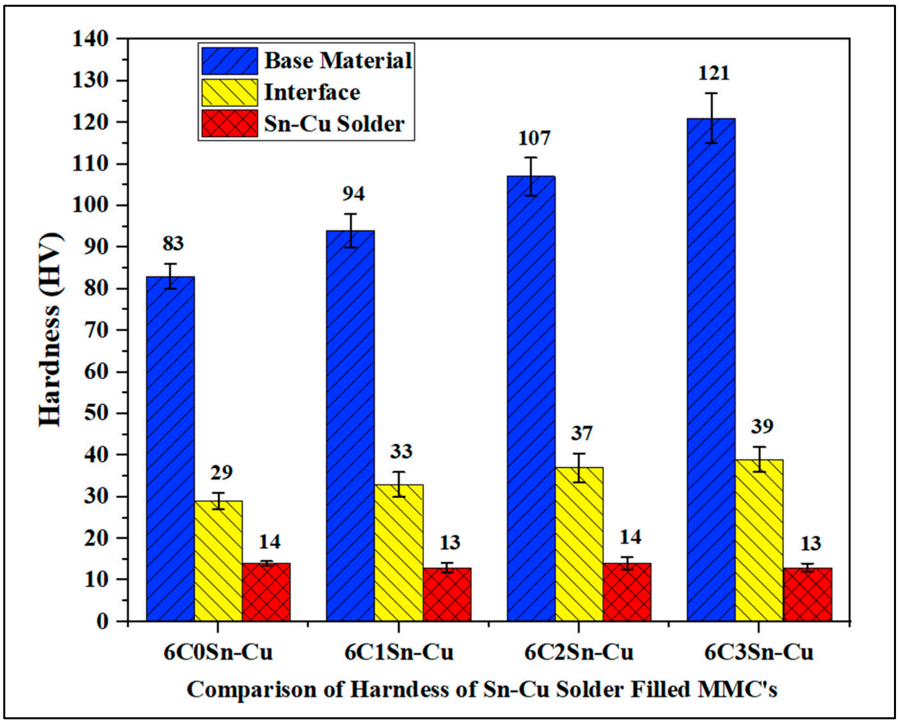

(**b**) Sn-Cu solder filled samples hardness

Figure 4. The hardness of Al6061-CuO MMCs filled with soldiers.

(**a**)

(**b**)

Figure 5. (**a**) Solder-filled tensile specimens and (**b**) Radiography of the solder-filled samples.

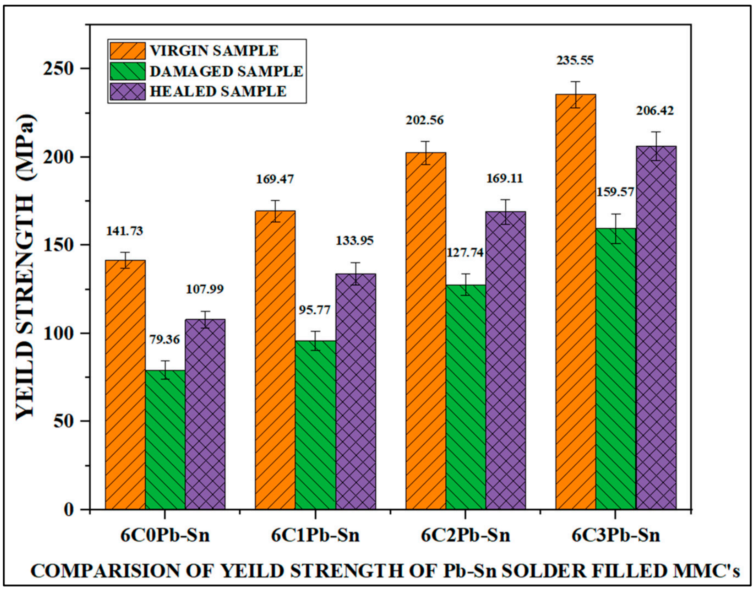

(**a**)

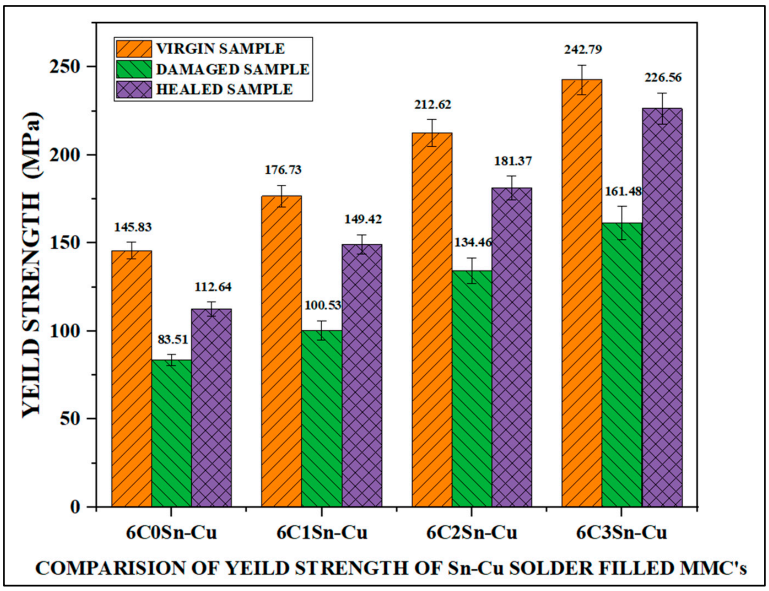

(**b**)

Figure 6. (**a**) The yield strength comparison of the Pb-Sn filled Al6061-CuO MMCs and (**b**) Sn-Cu filled Al6061-CuO MMCs.

The UTS for Pb-Sn reinforced samples for base alloy (6C0Pb-Sn) for the virgin test specimen is 154.90 MPa as compared to that of the self-healed sample is 131.14 MPa, the UTS for 6 wt.% of CuO (6C3Pb-Sn) reinforced virgin sample is 253.35 MPa and healed samples is 228.064 MPa the results are presented in the graph in Figure 7a. Whereas UTS for Sn-Cu reinforced samples with base alloy (6C0Sn-Cu) for the virgin test specimen is 160.28 MPa as compared to that of the self-healed sample is 137.70 MPa, the UTS for 6 wt.% of CuO (6C3Sn-Cu) reinforced virgin sample is 263.17 MPa and healed samples is 241.62 MPa the Figure 7b, is presented with the results. The standard deviation for UTS strength of Pb-Sn and Sn-Cu filled Al6061-CuO MMCs Sn-Cu solder was ±6.72 MPa.

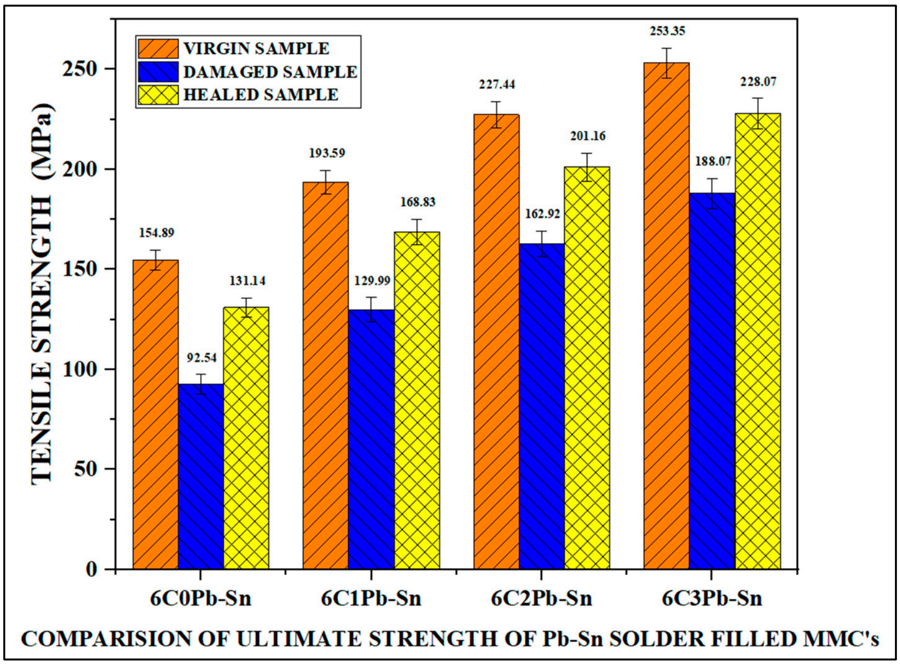

(**a**)

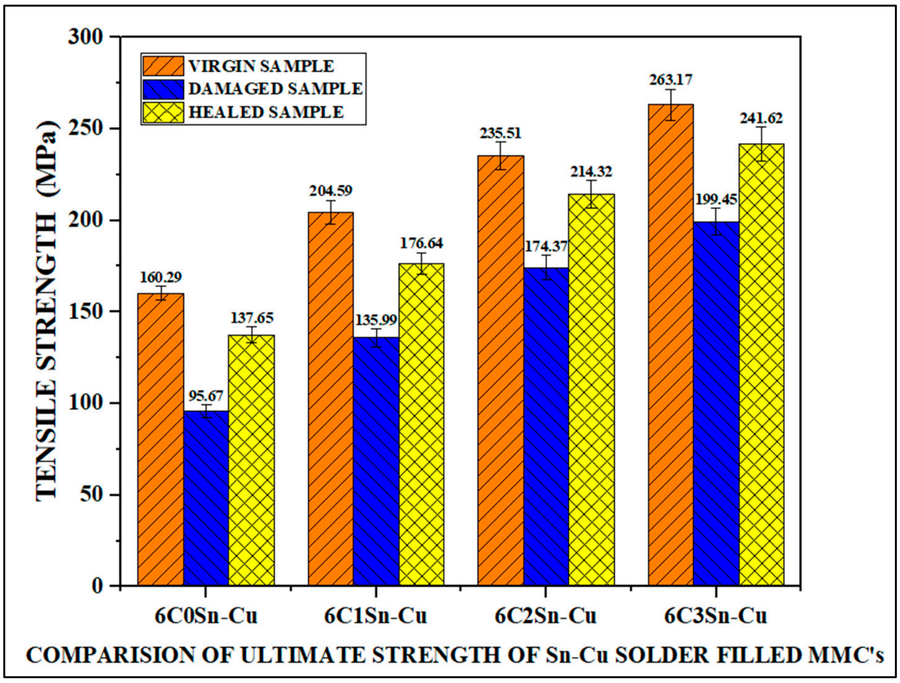

(**b**)

Figure 7. UTS comparison, (**a**) Pb-Sn filled Al6061-CuO MMCs and (**b**) Sn-Cu filled Al6061-CuO MMCs.

It is observed from Figure 8a that for Pb-Sn reinforced samples for base alloy (6C0Pb-Sn), the virgin sample has a strain of about 13.19% as compared to 11.26% that of the self-healed sample, the percentage elongation for 6 wt.% of CuO reinforced (6C3Sn-Cu) virgin sample and healed samples are 9.72% and 6.87% respectively. The standard deviation for percentage elongation of Pb-Sn solder was ±0.53%. However, for Sn-Cu reinforced samples for base alloy (6C0Sn-Cu), the virgin sample has a strain of 14.06%. In comparison, for 12.19% of the self-healed sample, the percentage elongation for 6 wt.% of CuO reinforced (6C3Sn-Cu) virgin sample and healed samples are 10.36% and 8.97%, respectively. The above graph and data show that the Sn-Cu solder will give less percentage elongation than the Pb-Sn solder. The standard deviation for percentage elongation of Pb-Sn solder was ±0.55%. The results are presented in the graph in Figure 8a,b.

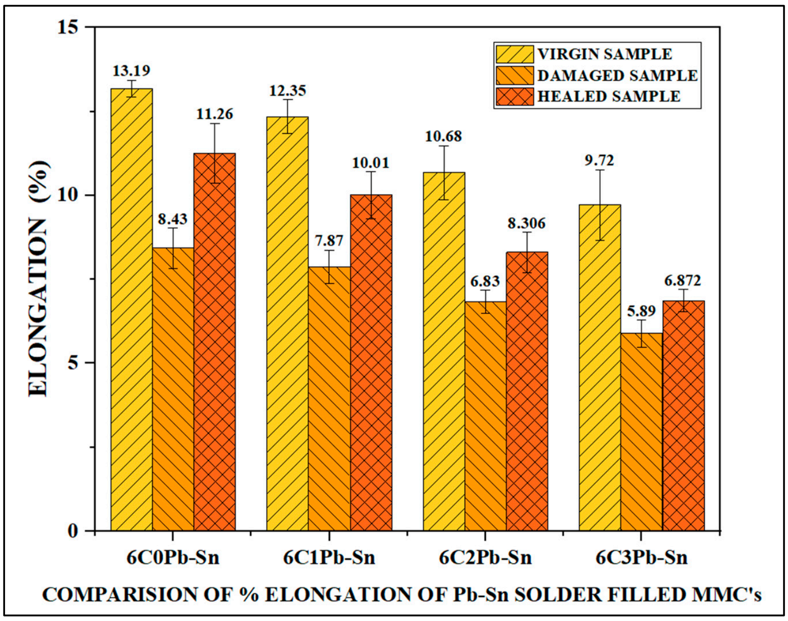

(**a**)

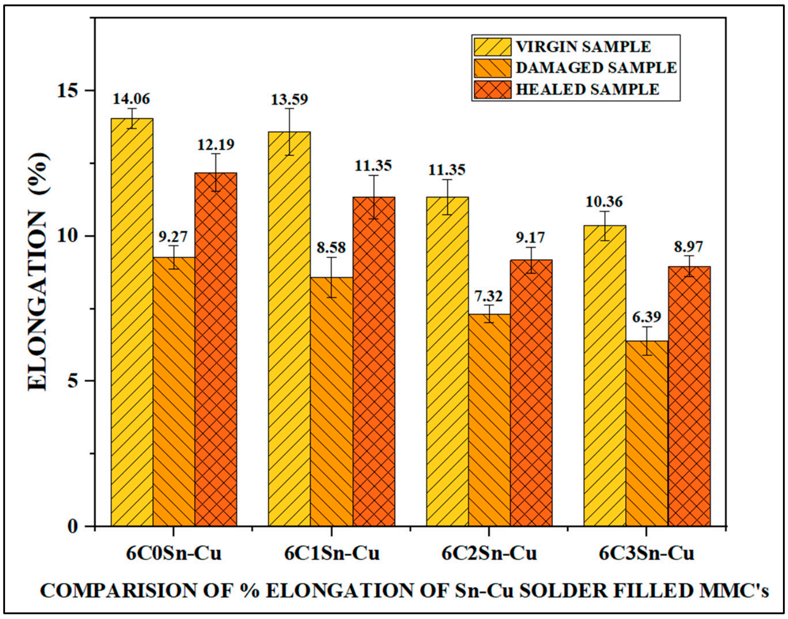

(**b**)

Figure 8. (**a**) % Elongation comparison of the Pb-Sn filled Al6061-CuO MMCs and (**b**) Sn-Cu filled Al6061-CuO MMCs.

The evaluated tensile characteristics of the Al6061 MMCs with self-healing material are depicted in Figures 6–8. The presented results show that incorporating Pb-Sn in Al6061 MMCs resulted in a lower UTS than that of samples reinforced with Sn-Cu solder by 11.09%, and the strain increased by 23.09%. The tensile properties of the Sn-Cu solder area are more significant than that of the Pb-Sn solder-filled area owing to the respectable bonding among solder and matrix. The alloy's poor tensile characteristics compromise the UTS of the MMC at the lower melting point. Also, improper load transmission through the bulk material is made possible by a deprived interfacial connection between the solder and the matrix. In the case of self-healing composite, this leads to poor tensile strength.

3.4. Impact Test Results for Samples Incorporated with Solders

The impact test samples were prepared per the literature, and solder filling is confirmed with radiography, as shown in Figure 9a–d. It has been noted that the samples that underwent self-healing treatment absorbed more impact energy than the damaged test samples that were untreated. The impact energy absorbed by the Pb-Sn reinforced samples for base alloy (6C0Pb-Sn) for the virgin test specimen is 10.05 J as compared to that of the self-healed sample is 8.8 J respectively, the impact energy absorbed for 6 wt.% of CuO (6C3Pb-Sn) reinforced virgin sample is 11.85 J and healed samples are 10.7 J the results are presented in the graph in Figure 9e. Further, the impact energy absorbed by Sn-Cu reinforced samples with base alloy (6C0Sn-Cu) for the virgin test specimen is 9.6 J as compared to that of the self-healed sample are 8.17 J, the impact energy absorbed by 6 wt.% of CuO (6C3Sn-Cu) reinforced virgin sample are 16.05 J and healed samples are 14.62 J the results are presented in the graph in Figure 9f.

(**a**) Impact specimens

(**b**) Solder-filled Impact specimens

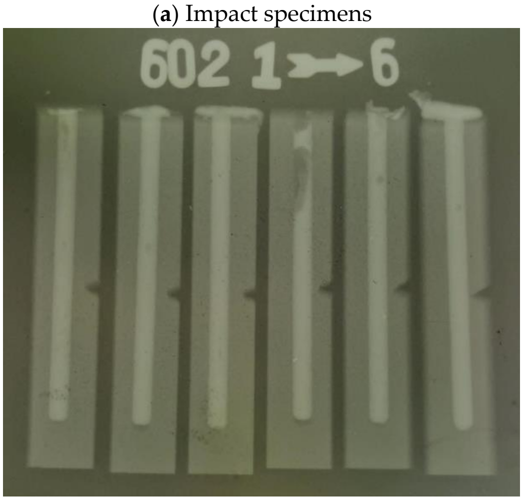

(**c**) Radiography of Solder-filled Impact specimens

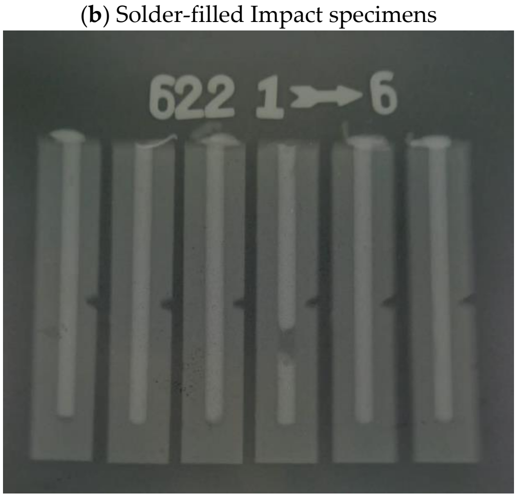

(**d**) Radiography of Solder-filled Impact specimens

Figure 9. *Cont.*

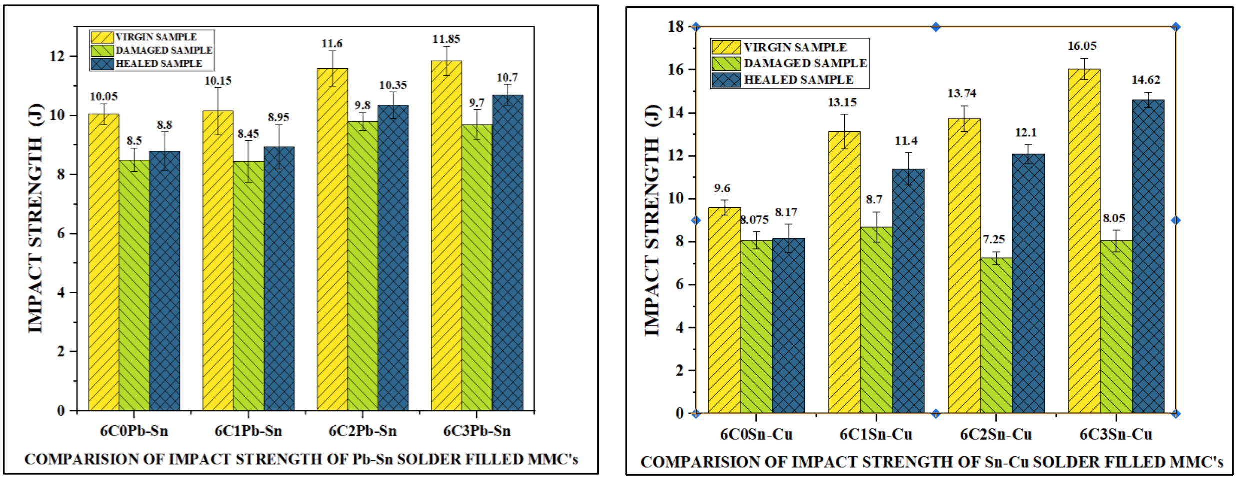

(e) (f)

Figure 9. (**a**) Impact specimens (**b**) Solder-filled impact specimens (**c**,**d**) Radiography of the impact samples (**e**,**f**) Impact strength of Al6061 alloy and Al6061-CuO MMCs filled with solders.

From the results presented in Figure 9e,f, it is noted that the incorporation of Pb-Sn in Al6061 MMCs' resulted in reduced energy absorbed than that of samples reinforced with Sn-Cu solder by 26.81%. The impact energy absorbed by the Sn-Cu solder is greater than that of the Pb-Sn solder-filled due to the good bonding between the solder and matrix. The standard deviation for impact strength of Pb-Sn solder and Sn-Cu solder based MMCs was ±0.62% and ±0.65% respectively.

3.5. Self-Healing Efficiency Comparision

Figure 10 shows that solder is appropriately filled into the composite bores, demonstrating the filling of the artificial crack (hole). The solder border and matrix are also easily discernible. After the temperature is applied, solder material enters the formed fissures. To improve the contact between Al6061 matrixes, solder material must be filled correctly. When exposed to high temperatures between 210 °C and 230 °C, the self-healing Al6061 and its CuO MMCs specimens with manufactured fissures filled the cracks, allowing solder to flow into them. The self-healing behaviour of MMCs' is validated in succession in Figure 10a–d. It was found that when the sample was held vertically, the solder filled the 2 mm hole when the temperature was applied, resulting in the resulting artificial fracture healing.

The evaluated tensile characteristics of the Al6061 MMCs with self-healing materials are tabulated in Tables 4 and 5, and the self-healing efficiency is calculated using Equation (1). It is evident that the highest self-healing efficiency for the composites filled with Pb-Sn is for 6 wt.%, composite is 90.02%, whereas the highest self-healing efficiency for the Sn-Cu filled composites is 6 wt.%. Composite is 91.81%. Where, T_{Virgin}, $T_{Damaged}$, T_{Healed}, are UTS of virgin, damaged and healed samples, respectively, and $\eta_{Self\ Healing-Tensile}$ is the healing efficiency of the tensile sample. It was shown that the samples that underwent self-healing treatment had a better UTS than the untreated damaged samples.

(**a**) Solder filled samples

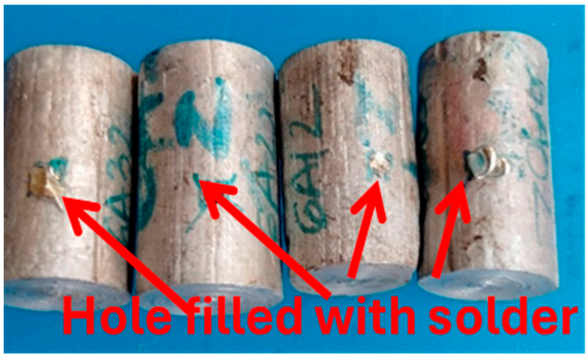

(**b**) Solder-filling artificial crack

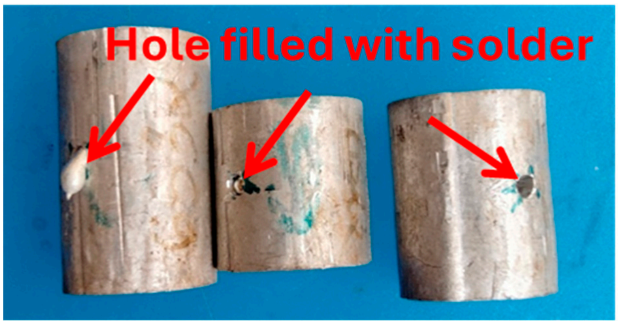

(**c**) Solder filling the artificial crack.

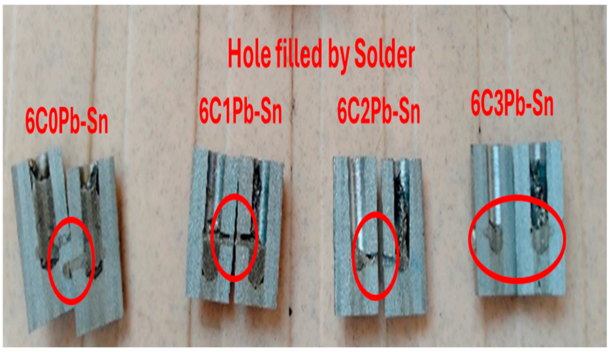

(**d**) Cut section samples after the Self-healing test.

(**e**) Tensile Virgin specimen

(**f**) Impact specimen Self-healed

Figure 10. Al6061-CuO MMCs filled with Solders after self-healing treatment.

The reinforcing of the low melting point alloy causes the Al6061 to lose its tensile characteristics. The tensile strength of self-healing MMCs is decreased by the low melting point alloy's weak tensile properties. Furthermore, inadequate interfacial contact between the solder material, reinforcement, and Al matrix hinders adequate load transfer through the bulk material. However, the alloy's low melting point prevents the sample from breaking in two.

Table 4. Tensile Strength of the samples filled with Pb-Sn solder.

Samples	T_{Virgin} (Mpa)	$T_{Damaged}$ (Mpa)	T_{Healed} (Mpa)	$\eta_{Self\ Healing\ -\ Tensile}$ (%)
6C0Pb-Sn	154.90	92.54	131.14	84.7
6C1Pb-Sn	193.58	129.99	168.83	87.2
6C2Pb-Sn	227.44	162.92	201.16	88.4
6C3Pb-Sn	253.35	188.06	228.06	90.0

Table 5. Tensile Strength of the samples filled with Sn-Cu solder.

Samples	T_{Virgin} (Mpa)	$T_{Damaged}$ (Mpa)	T_{Healed} (Mpa)	$\eta_{Self\ Healing\ -\ Tensile}$ (%)
6C0Sn-Cu	154.90	92.54	131.14	84.66
6C1Sn-Cu	204.58	135.99	176.64	86.34
6C2Sn-Cu	235.51	174.37	214.32	91.00
6C3Sn-Cu	263.17	199.45	241.62	91.81

Tables 6 and 7 present the energy absorbed during impact testing by Pb-Sn and Sn-Cu solder-filled composite samples. According to the results, the highest self-healing efficiency (according to Equation (1)) for Pb-Sn filled composites is observed at 6C3Pb-Sn, i.e., 90.30%, whereas for Sn-Cu filled composites, the highest is observed for 6C3Sn-Cu, i.e., 91.09%.

Table 6. Impact strength of the samples filled with Pb-Sn solder.

Samples	T_{Virgin} (Mpa)	$T_{Damaged}$ (Mpa)	T_{Healed} (Mpa)	$\eta_{Self\ Healing\ -\ Tensile}$ (%)
6C0Pb-Sn	10.05	8.5	8.8	87.56
6C1Pb-Sn	10.15	8.45	8.95	88.18
6C2Pb-Sn	11.6	9.8	10.35	89.22
6C3Pb-Sn	11.85	9.7	10.7	90.30

Table 7. Impact strength of the samples filled with Sn-Cu solder.

Samples	T_{Virgin} (Mpa)	$T_{Damaged}$ (Mpa)	T_{Healed} (Mpa)	$\eta_{Self\ Healing\ -\ Tensile}$ (%)
6C0Sn-Cu	9.6	8.075	8.17	85.10
6C1Sn-Cu	13.15	8.7	11.4	86.69
6C2Sn-Cu	13.74	7.25	12.1	88.06
6C3Sn-Cu	16.05	8.05	14.62	91.09

Where, E_{Virgin}, $E_{Damaged}$, E_{Healed}, are energy absorbed by the sample in impact testing of a virgin, damaged and healed samples, respectively, and $\eta_{Self\ Healing-Imapct}$. A wide range of variables can influence the performance or characteristics of a composite. It becomes harder to compare composite results directly from different sources because of factors such as the manufacturing process, kind of reinforcement, and reinforcement mix ratios. The way that Al6061 interacts with filled solder material explains this phenomenon. Due to this weak contact barrier, the Al6061 alloy's applied load cannot propagate into the metal. The stress concentration caused by the sample's 3 mm hole is also important. Analysis of the unsuccessful specimens revealed that impact energy frequently splits the sample in two, but even after fracture, the samples in the self-healing MMCs' maintain their integrity, as seen in Figure 10e,f.

The healing efficacy of this process is promising, as revealed by Alaneme and Omusule [26], Oladijo et al. [36], and several other investigational studies [34,37–40]. This procedure restores strength to at least 60% of its pre-damage level. It is important to recognize that this healing process is successful because of the wettability of the alloy with the low melting temperature and the metallic substance. Differences in the interfacial bonding between the materials under study might cause variations in the healing efficiencies achieved. Figure 11a,b compare healing efficiencies of tensile and impact samples of Pb-Sn-filled Al6061-CuO MMCs and Sn-Cu-filled Al6061-CuO MMCs.

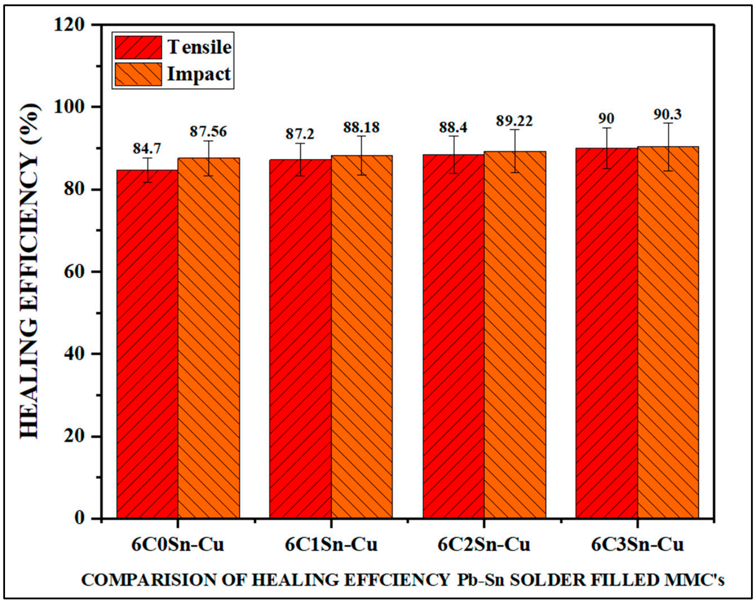

(**a**)

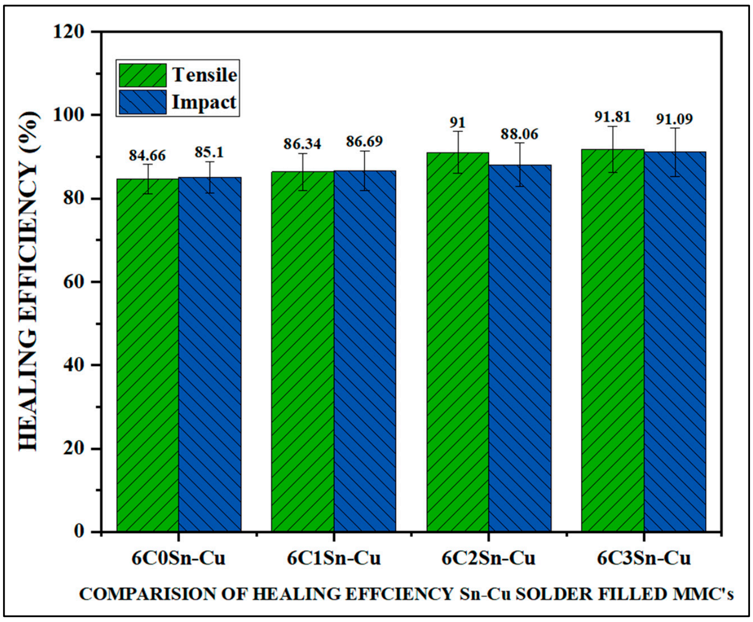

(**b**)

Figure 11. Healing Efficiencies of tensile and impact samples. (**a**) comparison of Pb-Sn filled Al6061-CuO MMCs and (**b**) comparison of Sn-Cu filled Al6061-CuO MMCs.

The interaction between primary and secondary reinforcements, which is not considered in this paper, might be the reason for the low energy absorbed. For example, the interaction may have impacted the interfacial bonding between the Al6061-CuO reinforced composites and the Pb-Sn and Sn-Cu low melting point alloys, leading to poor healing efficiencies. Because various materials have varied healing features, it is crucial to take notice of the challenges associated with applying a healing approach from one material to another. Even though the efficiency of composites' healing is higher, the reinforcing elements are crucial in lowering the alloy's healing efficiency. The standard deviation for healing efficiency of Pb-Sn and Sn-Cu filled Al6061-CuO MMCs was ±2.65% and 2.73% respectively.

4. Conclusions

The effects of adding different quantities of submicron-CuO particles to Al6061 MMCs were examined in this work utilizing a modified liquid metallurgical technique that included ultrasonication and secondary reinforcement of Pb-Sn and Sn-Cu solder separately. The goal was to ascertain the benefits of using a low melting point alloy and assess its capacity for self-healing. The significant features of the work are as follows. It is evident from the micrographs that a decent bond is formed between solder and matrix, which confirms the successful fabrication of composites. Compared to virgin samples and samples containing 6% weight of CuO (6C3Pb-Sn), Pb-Sn reinforced self-healed samples exhibit a greater healing efficiency in both tension and impact loading conditions. Compared to virgin samples and samples containing 6% weight of CuO (6C3Sn-Cu), the study shows that Sn-Cu reinforced self-healed samples had a greater healing efficiency in both tension and impact loading conditions. This encourages research on using different solders to get higher healing efficiency.

Author Contributions: S.R.V.M.: Project administration, Methodology, Investigation, Formal analysis, Data curation, Conceptualization. G.B.V.K.: Writing—review & editing, MProject administration, Methodology, Investigation, Formal analysis, Data curation, Conceptualization. R.P.: Writing—original draft, Visualization, Validation, Data Analysis, Supervision, Software, Resources. C.S.P.R.: Project administration, Methodology, Investigation. M.S.S.: Project administration, Methodology and funding. S.K.S.: Project administration and data curation All authors have read and agreed to the published version of the manuscript.

Funding: No funding was received for this work.

Data Availability Statement: The data presented in the article are original findings and will be made available to the reader upon the request to the corresponding author.

Acknowledgments: With deep appreciation, the authors thank the NIT, Andhra Pradesh, VIIT(A)-Andhra Pradesh Amrita Vishwa Vidyapeetham, Bengaluru Campus, NIT, Warangal, Robert Gordon University, UK and VIT-Andhra Pradesh.

Conflicts of Interest: The authors affirm that none of their personal connections or apparent conflicting financial interests could have influenced the findings of this study.

References

1. Das, D.K.; Mishra, P.C.; Singh, S.; Thakur, R.K. Properties of Ceramic-Reinforced Aluminium Matrix Composites—A Review. *Int. J. Mech. Mater. Eng.* **2014**, *9*, 1–16. [CrossRef]
2. Maddaiah, K.C.; Veeresh Kumar, G.B.; Pramod, R. Studies on the Mechanical, Strengthening Mechanisms and Tribological Characteristics of AA7150-Al_2O_3 Nano-Metal Matrix Composites. *J. Compos. Sci.* **2024**, *8*, 97. [CrossRef]
3. Lyu, M.-Y.; Choi, T.G. Research Trends in Polymer Materials for Use in Lightweight Vehicles. *Int. J. Precis. Eng. Manuf.* **2015**, *16*, 213–220. [CrossRef]

4. Rao, T.B. An Experimental Investigation on Mechanical and Wear Properties of Al7075/SiCp Composites: Effect of SiC Content and Particle Size. *J. Tribol.-Trans. ASME* **2018**, *140*, 031601. [CrossRef]
5. Gouda, S.; Veeresh Kumar, G.B.; Pramod, R.; Prasanna, N.D.; Balasubramanya, H.S.; Aradhya, S.M. Fabrication, Mechanical and Wear Properties of Aluminum (Al6061)-Silicon Carbide-Graphite Hybrid Metal Matrix Composites. *Frat. Integrità Strutt.* **2022**, *16*, 134–149. [CrossRef]
6. Dasgupta, R. Aluminium Alloy-Based Metal Matrix Composites: A Potential Material for Wear-Resistant Applications. *Int. Sch. Res. Not.* **2012**, *2012*, 594573. [CrossRef]
7. Samal, P.; Vundavilli, P.R.; Meher, A.; Mahapatra, M.M. Recent Progress in Aluminum Metal Matrix Composites: A Review on Processing, Mechanical, and Wear Properties. *J. Manuf. Process.* **2020**, *59*, 131–152. [CrossRef]
8. Gök, D.A.; Bayraktar, C.; Hoskun, M. A Review on Processing, Mechanical, and Wear Properties of Al Matrix Composites Reinforced with Al_2O_3, SiC, B_4C, and MgO by Powder Metallurgy Method. *J. Mater. Res. Technol.* **2024**, *31*, 1132–1150. [CrossRef]
9. Mourad, A.-H.I.; Christy, J.V.; Krishnan, P.K.; Mozumder, M.S. Production of Novel Recycled Hybrid Metal Matrix Composites Using Optimized Stir Squeeze Casting Technique. *J. Manuf. Process.* **2023**, *88*, 45–58. [CrossRef]
10. Kandpal, B.C.; Kumar, J.; Singh, H. Manufacturing and Technological Challenges in Stir Casting of Metal Matrix Composites—A Review. *Mater. Today Proc.* **2018**, *5*, 5–10. [CrossRef]
11. Torralba, J.M.; da Costa, C.E.; Velasco, F. P/M Aluminium Matrix Composites: An Overview. *J. Mater. Process. Technol.* **2003**, *133*, 203–206. [CrossRef]
12. Hashim, J.; Looney, L.; Hashmi, M.S.J. Metal Matrix Composites: Production by the Stir Casting Method. *J. Mater. Process. Technol.* **1999**, *92–93*, 1–7. [CrossRef]
13. Bodunrin, M.O.; Alaneme, K.K.; Chown, L.H. Aluminium Matrix Hybrid Composites: A Review of Reinforcement Philosophies; Mechanical, Corrosion, and Tribological Characteristics. *J. Mater. Res. Technol.* **2015**, *4*, 434–445. [CrossRef]
14. Hashim, J.; Looney, L.; Hashmi, M.S.J. Particle Distribution in Cast Metal Matrix Composites—Part I. *J. Mater. Process. Technol.* **2002**, *123*, 251–257. [CrossRef]
15. Hashim, J.; Looney, L.; Hashmi, M.S.J. The Enhancement of Wettability of SiC Particles in Cast Aluminium Matrix Composites. *J. Mater. Process. Technol.* **2001**, *119*, 329–335. [CrossRef]
16. Alaneme, K.K.; Omosule, O.I. Experimental Studies of Self-Healing Behaviour of Under-Aged Al-Mg-Si Alloys and 60Sn-40Pb Alloy Reinforced Aluminium Metal Matrix Composites. *J. Miner. Mater. Charact. Eng.* **2015**, *3*, 1–8. [CrossRef]
17. Amano, R.; Rohatgi, P.; Lucci, J.M.; Schultz, B.; Ruzek, A. Design and Demonstration of Self-Healing Behavior in a Lead-Free Solder Alloy. In Proceedings of the 7th International Energy Conversion Engineering Conference, Denver, CO, USA, 2–5 August 2009. AIAA 2009-4514.
18. Egan, P.; Sinko, R.; Leduc, P.R.; Ketan, S. The role of mechanics in biological and bio-inspired systems. *Nat. Commun.* **2015**, *6*, 7418. [CrossRef]
19. Ferguson, J.B.; Schultz, B.F.; Rohatgi, P.K. Self-Healing Metals and Metal Matrix Composites. *JOM* **2014**, *66*, 866–871. [CrossRef]
20. Ghosh, S.K. *Self-Healing Materials: Fundamentals, Design Strategies, and Applications*; John Wiley & Sons: Hoboken, NJ, USA, 2009. [CrossRef]
21. Schmets, A.J.M.; van der Zaken, G.; Van der Zwaag, S. *Self Healing Materials: An Alternative Approach to 20 Centuries of Materials Science*; Van der Zwaag, S., Ed.; Springer: Dordrecht, The Netherlands, 2007. [CrossRef]
22. Hager, M.D.; Greil, P.; Leyens, C.; van der Zwaag, S.; Schubert, U.S. Self-healing materials. *Adv. Mater.* **2010**, *22*, 5424–5430. [CrossRef]
23. Blaiszik, B.J.; Kramer, S.L.B.; Olugebefola, S.C.; Moore, J.S.; Sottos, N.R.; White, S.R. Self-healing polymers and composites. *Annu. Rev. Mater. Res.* **2010**, *40*, 179–211. [CrossRef]
24. Urdl, K.; Kandelbauer, A.; Kern, W.; Müller, U.; Thebault, M.; Zikulnig-Rusch, E. Self-healing of densely crosslinked thermoset polymers—A critical review. *Prog. Org. Coat.* **2017**, *104*, 232–249. [CrossRef]
25. Nakao, W.; Takahashi, K.; Ando, K. Self-healing of surface cracks in structural ceramics. In *Advanced Nanomaterials*; Wiley-VCH: Weinheim, Germany, 2010; pp. 555–593. [CrossRef]
26. Madhankumar, M.; Prabhakaran, G.V. Self-healing ability of structural ceramics—A review. In *Trends in Intelligent Robotics, Automation, and Manufacturing, Proceedings of the First International Conference, Kuala Lumpur, Malaysia, 28–30 November 2012*; Ponnambalam, S.G., Parkkinen, J., Ramanathan, K.C., Eds.; Springer: Berlin/Heidelberg, Germany, 2012; pp. 466–474.
27. Alaneme, K.K.; Bodunrin, M.O. Self-healing using metallic material systems—A review. *Appl. Mater. Today* **2017**, *6*, 9–15. [CrossRef]
28. Manuel, M.V.; Olson, G.B. Biomimetic self-healing metals. In Proceedings of the 1st International Conference on Self-Healing Materials, Noordwijk aan Zee, The Netherlands, 18–20 April 2007.
29. Bodunrin, M.O.; Oladijo, O.P.; Daramola, O.O.; Alaneme, K.K.; Maledi, N.B. Porosity measurement and wear performance of aluminium hybrid composites reinforced with silica sand and bamboo leaf ash. *Ann. Fac. Eng. Hundeoara Int. J. Eng.* **2016**, *16*, 232–238.

30. Guadagno, L.; Naddeo, C.; Raimondo, M.; Barra, G.; Vertuccio, L.; Sorrentino, A.; Binder, W.H.; Kadlec, M. Development of self-healing multifunctional materials. *Compos. Part B Eng.* **2017**, *128*, 30–38. [CrossRef]
31. Ferguson, J.B.; Schultz, B.F.; Rohatgi, P.K. Zinc alloy ZA-8/shape memory alloy self-healing metal matrix composite. *Mater. Sci. Eng. A* **2015**, *620*, 85–88. [CrossRef]
32. Karabulut, Ş.; Karakoç, H.; Bilgin, M.; Canpolat, B.H.; Krolczyk, G.; Sarıkaya, M. A Comparative Study on Mechanical and Ballistic Performance of Functionally Graded Al6061 Composites Reinforced with B_4C, SiC, and Al_2O_3. *J. Mater. Res. Technol.* **2023**, *23*, 5050–5065. [CrossRef]
33. Mantha, S.R.V.; Kumar, G.B.V.; Pramod, R.; Rao, C.S.P. Investigations on Microstructure, Mechanical, and Wear Properties, with Strengthening Mechanisms of Al6061-CuO Composites. *J. Manuf. Mater. Process.* **2024**, *8*, 245. [CrossRef]
34. Nosonovsky, M.; Rohatgi, P.K. *Biomimetics in Materials Science: Self-Healing, Self-Lubricating and Self-Cleaning Materials*; Springer Series in Materials Science; Springer: New York, NY, USA, 2012; Volume 152, pp. 53–73. [CrossRef]
35. Lucci, J.M.; Amano, R.S.; Rohatgi, P.; Schultz, B. Self-Healing in an Aluminum Alloy Reinforces with Microtubes. In Proceedings of the ASME 2008 3rd Energy Nanotechnology International Conference Collocated with the Heat Transfer, Fluids Engineering, and Energy Sustainability Conferences, Jacksonville, FL, USA, 10–14 August 2008; ASME: New York, NY, USA, 2008; pp. 79–88. [CrossRef]
36. Oladijo, O.P.; Bodunrin, M.O.; Sobiyi, K.; Maledi, N.B.; Alaneme, K.K. Investigating the self-healing behaviour of under-aged and 60Sn-40Pb alloy reinforced aluminium hybrid composites. *Thin Solid Film.* **2016**, *620*, 201–205. [CrossRef]
37. Sanada, K.; Yasuda, I.; Shindo, Y. Transverse tensile strength of unidirectional fibre-reinforced polymers and self-healing of interfacial debonding. *Plast. Rubber Compos.* **2006**, *35*, 67–72. [CrossRef]
38. Lucci, J.M.; Amano, R.S.; Rohatgi, P.; Schultz, B. Experiment and computational analysis of self-healing in an aluminium alloy. In Proceedings of the 2008 ASME International Mechanical Engineering Congress and Exposition, Boston, MA, USA, 31 October–6 November 2008; pp. 1–10.
39. Srivastava, V.; Gupta, M. Impact of Post Hardening Mechanism on Self-Healing Assessment of AA2014 Nitinol-Based Smart Composites. *Met. Mater. Int.* **2021**, *27*, 2666–2681. [CrossRef]
40. Lucci, J.M.; Amano, R.S.; Rohatgi, P.K. Heat transfer and fluid flow analysis of self-healing in metallic materials. *Heat Mass Transf.* **2016**, *53*, 825–848. [CrossRef]